HHS Public Access

Author manuscript

Neurobiol Aging. Author manuscript; available in PMC 2023 April 01.

Published in final edited form as:

Neurobiol Aging. 2022 April ; 112: 87–101. doi:10.1016/j.neurobiolaging.2021.11.009.

Alpha desynchronization during Stroop test unmasks cognitively healthy individuals with abnormal CSF Amyloid/Tau

Xianghong Arakaki, MD, PhD[a], **Shao-Min Hung, PhD**[a,b], **Roger Rochart**[a], **Alfred N. Fonteh, PhD**[a], **Michael G. Harrington, MB, ChB, FRCP**[c]

[a]Neurosciences, Huntington Medical Research Institutes, Pasadena, CA

[b]Division of Biology and Biological Engineering, California Institute of Technology, Pasadena, CA

[c]Department of Neurology, University of Southern California, Los Angeles, CA, USA

Abstract

Synaptic dysfunctions precede cognitive decline in Alzheimer's disease (AD) by decades, affect executive functions, and can be detected by quantitative electroencephalography (qEEG). We used qEEG combined with Stroop testing to identify changes of inhibitory controls in cognitively healthy individuals with an abnormal versus normal ratio of cerebrospinal fluid (CSF) amyloid/total-tau. We studied two groups of participants (60–94 years) with either normal (CH-NAT or controls, n = 20) or abnormal (CH-PAT, n = 21) CSF amyloid/tau ratio. We compared: alpha event-related desynchronization (ERD), alpha spectral entropy (SE), and their relationships with estimated cognitive reserve. CH-PATs had more negative occipital alpha ERD, and higher frontal and occipital alpha SE during low load congruent trials, indicating hyperactivity. CH-PATs demonstrated fewer frontal SE changes with higher load, incongruent Stroop testing. Correlations of alpha ERD with estimated cognitive reserve were significant in CH-PATs but not in CH-NATs. These results suggested compensatory hyperactivity in CH-PATs compared to CH-NATs. We did not find differences in alpha ERD comparisons with individual CSF amyloid(A), p-tau(T), total-tau(N) biomarkers.

Corresponding author: Xianghong Arakaki, Neurosciences, Huntington Medical Research Institutes, 686 S. Fair Oaks Ave., Pasadena, CA 91105, xianghong@hmri.org.

Author Contributions

Conception and design of the study: XA MGH. Acquisition of the data: XA MGH. Analysis of the data: XA SMH RR AF MGH. Wrote the paper, XA. Edited the paper: XA SMH RR AF MGH. All authors contributed toward discussions of the results and the final manuscript.

Credit Author Statement:

Conception and design of the study: XA MGH. Acquisition of the data: XA MGH. Analysis of the data: XA SMH RR AF MGH. Wrote the paper, XA. Edited the paper: XA SMH RR AF MGH. All authors contributed toward the final manuscript.

Conflicts of Interest

No conflicts.

Keywords

CH-PATs; CH-NATs; electroencephalography; Stroop; alpha event-related desynchronization; spectral entropy

1. Introduction

Neuropathology and biomarkers of Alzheimer's disease (AD) demonstrate that synaptic dysfunction and pathology (amyloid/tau) precede cognitive impairment by decades (Harari et al., 2014; Nathan et al., 2017) and can be detected by resting electroencephalography (EEG) (Babiloni et al., 2020a). The lack of effective AD treatment requires efforts to identify early pathology and predict clinical decline in late-onset AD(Cummings et al., 2019). The US National Institute on Aging–Alzheimer's Association (NIA-AA) updated scientific progress and unified the 2011 guidelines as a "research framework"(Jack et al., 2018). This research framework classifies AD and AD related dementia spectrum based on ATN status, where A+ pathology is the main AD pathology. The framework envisions combinations of AD biomarkers that can help understand AD progression before cognitive symptoms appear and encourages investigation of the interaction between amyloid/tau biomarkers and cognitive symptoms (Jack et al., 2018).

Previous studies by our group and others demonstrated decreased inhibitory control in AD, using Stroop interference testing (Harrington et al., 2013; Tissier et al., 2018; van Veen and Carter, 2005). The classic Stroop color-naming task, where participants are asked to name the color of the ink in which a word is printed while ignoring the word itself, has been used to test one core executive function - interference, selective attention, and goal maintenance. Stroop performance is impaired in preclinical AD, mild cognitive impairment (MCI), and AD(Belanger et al., 2010; Patten et al., 2018; Tse et al., 2010). FMRI study of the prefrontal cortex during Stroop reported hyperactivity in MCI and hypoactivity in AD compared to elderly controls (Li et al., 2009). With higher temporal resolution, complementary EEG techniques identified changes of alpha power or event-related activities during interference tests in frontal and posterior areas (Jiang et al., 2015; Larson et al., 2009; Nombela et al., 2014). Interestingly, during resting state, several studies reported altered frontal and occipital alpha activity: reduced occipital alpha activity in EEG studies of progressive MCI or AD(Babiloni et al., 2015; Bajo et al., 2012); frontal alpha power augmentation related to local amyloid deposition in magnetoencephalography (MEG) in predementia stages of AD(Nakamura et al., 2018). Further, EEG during Stroop testing highlighted the frontal and occipital alpha involved in the interaction between stimulus and age, the best-known risk factor for AD(Nombela et al., 2014). On the other hand, during cognitive challenge, alpha event-related desynchronization (ERD) and spectral entropy (SE) were considered as functional correlates of brain activation(Inouye et al., 1991; Klimesch, 2012; Klimesch et al., 2007; Nunes et al., 2004). Cognitively healthy individuals with pathological amyloid/tau (CH-PATs) demonstrated decreased (more negative) alpha ERD and greater alpha SE during working memory testing, indicating hyperactivity compared to those with normal amyloid/tau(Arakaki et al., 2019). Since working memory is related to Stroop interference

processing(Jaiswal et al., 2019), we predict that altered alpha ERD and SE during Stroop testing will reveal individuals with CH-PAT biomarkers.

Cognitive reserve has been reported to account for inter-individual differences in cognitive symptomatic onset from aging or neurodegenerative pathology(Stern, 2009). Cognitive reserve can be estimated by proxies of education years and verbal IQ(Frankenmolen et al., 2018; Narbutas et al., 2019). Higher cognitive reserve has been related to resilience to cognitive decline from white matter lesions(Giogkaraki et al., 2013; Mortamais et al., 2014). To our knowledge, no other studies correlate cognitive reserve with alpha ERD.

Our goal for this study was to test whether frontal and occipital alpha ERD and SE during Stroop interference challenge is differentially altered in CH-PATs. As amyloid/tau ratio outperforms amyloid or tau alone (Fagan et al., 2011; Ritchie et al., 2017; Roe et al., 2013), we focused our alpha ERD and SE analysis based on CSF amyloid/tau ratio, which can include both AD type and non-AD type pathology. In a four year follow up, none of the CH-NATs but 40% of the CH- PATs declined cognitively (Harrington et al., 2013; Harrington et al., 2019; Wilder et al., 2018), evidence that the CH-PAT have greater risk of cognitive decline.

We also explored the alpha ERD changes on individual ATN biomarkers. Based on the observations of hyperactivity in an early stage of disease (Arakaki et al., 2019; Li et al., 2009; Nakamura et al., 2018), our hypotheses are that compared to CH-NATs during Stroop testing, CH-PATs will present: 1) decreased (more negative) alpha ERD at frontal and/or occipital regions; 2) higher frontal/occipital alpha SE and reduced changes in alpha SE from congruent to incongruent trials at the frontal/occipital regions.

This study uses cognitive challenge with objective measures of central (qEEG) to understand potential interference processing dysfunction in CH-PATs. Our results are the first to provide a template strategy and set of objective measures to detect early Alzheimer’s changes that correlate with invasive biomarkers (CSF amyloid/tau) and perhaps to assess potential efficacy of preventive treatments for cognitively healthy individuals, however we do plan additional studies to further validate and extend our methodology.

2. Participants and Methods

2.1. Participants

Fifty cognitively healthy elderly participants were recruited from advertisements placed in local newspapers and newsletters, the Pasadena Huntington Hospital Senior Health Network, the Pasadena Senior Center, and meetings with local physicians to present this research. All participants provided consent via an Institutional Review Board (IRB) approved protocol (HMRI # 33797). Assessments included collecting demographic data, physical exams, fasting blood studies, disease severity and disability scales, and CSF amyloid/tau measurements(Harrington et al., 2013). Inclusion criteria: over 60 years, classified as CH after a ~4 hour comprehensive neuropsychological battery using age, sex, and education normative references, including the Wechsler Adult Intelligence Scale–Third Edition (WAIS-III), from which the verbal IQ was estimated, Clinical Dementia Rating

(CDR), Montreal Cognitive Assessment (MoCA), and Mini Mental State Examination (MMSE), as referenced in detail (Harrington et al., 2013). Exclusion criteria: other active, untreated disease, use of anticoagulants or other contraindications to lumbar puncture. To reduce chronobiological variability of amyloid(Bateman et al., 2007), we collected all CSF between 8 and 10 am after a 12 h overnight fast.

CSF amyloid $A\beta_{42}$ and phospho-tau—CSF proteins were measured as published (Montagne et al., 2020). Briefly, we used the MSD multiplex assay (Cat. No. K15200E, MSD, Rockville, MD) to determine CSF levels of $A\beta_{42}$; participants were stratified based on CSF analysis as either $A\beta_{1–42}$-positive ($A\beta_{1–42}$+, <190 pg/mL) or $A\beta_{1–42}$-negative (Aβ−, >190 pg/mL) using the accepted cutoff values as previously reported for the MSD 6E10 Aβ peptide assay (Pan et al., 2015). We determined phosphorylated tau (pT181) by ELISA (Cat. No. 81581, Innotest, Belgium); participants were stratified based on CSF analysis as either $pTau_{181}$-positive (pTau+, >78 pg/mL) or $pTau_{181}$-negative (pTau−, <78 pg/mL), using the accepted cutoff value as previously reported (Roe et al., 2013).

CSF amyloid/total tau ratio—We previously used Aβ/total tau ratios to differentiate between individuals with normal versus abnormal CSF (Harrington et al., 2013) because these ratios had outperformed any single analyte in discriminating individuals with, versus without, abnormal levels of cortical amyloid (Fagan et al., 2011). We found a cutoff for the ratio of $Aß_{42}$/total tau (2.7132) provided at least 85% sensitivity in discriminating AD from CH participants; we then used this regression to assign cognitively healthy participants (CH) into two groups, one with normal CSF Aβ/tau ratio (CH-NATs) and the other with abnormal Aβ/tau ratio (CH-PATs) (Harrington et al., 2013). As provisional evidence for the capacity of this CSF Aβ/total tau ratio to predict clinical decline, a longitudinal study found that 40% of CH-PATs declined cognitively over 4 years, ranging from significant impairment, to MCI, or to AD, while none of the CH-NATs declined over 4 years (Harrington et al., 2019). The Innotest immunoassay used for this published amyloid/tau ratio (Innogenetics, Gent, Belgium) is, however, no longer available and, to overcome this, we compared data from 35 samples run on both Innotest and MSD platforms, using the MSD assay (catalog no. K15121G, MSD, Rockville, MD) to determine total tau (cutoff value >450 pg/mL) (Pan et al., 2015) along with the aforementioned MSD $A\beta_{42}$ assay; regression analysis (Fig. S1) allowed us to estimate Innotest values (reported in the Results section) for amyloid and total tau on these new samples run only on the current MSD platform.

CSF/EEG analyses—We compared participants in three approaches: 1) we compared the estimated CH-NAT to the CH-PAT group; 2) we compared the group with $A\beta_{42}$ <190 pg/mL (A+ for AD biomarker) to those with all normal CSF biomarkers for $A\beta_{42}$, p-Tau, and total Tau (A−T−N−); 3) we compared the group with any combination of abnormal ATN biomarker: $A\beta_{42}$ <190 pg/mL, or pTau+>78 pg/mL, or total tau>450 pg/mL (ATN(+)) to those with all normal CSF CSF biomarkers $A\beta_{42}$, p-Tau, and total Tau (A−T−N−).

2.2. Procedures

All study participants were seated in a quiet illuminated room under similar constant conditions and were first asked, during resting state baseline measures, to “sit still” and

"empty their minds" for 5 minutes with eyes open (eyes fixed at the DELL sign on the bottom of the dark screen), and then for 5 minutes with eyes closed. All participants were in a quiet awake state during the resting state condition.

We administered the Stroop interference test using E-prime software (Psychology Software Tools, Inc., Sharpsburg PA) on a Dell Precision T5610 with a 20" screen. Participants were comfortably seated in front of the computer screen. One of the three colored words 'Red', 'Blue,' or 'Green' presented on the screen one at a time in three different colors (red, blue, or green). The ink color and word can be congruent ("C", e.g., 'Red' in red ink) or incongruent ("I", e.g., 'Red' in blue ink). The researcher instructed participants to respond to the color of the ink and ignore the word using their right hand: press '1' for 'red', '2' for 'blue', and '3' for 'green' on a keyboard. Each trial was composed of a pre-set duration of 500 ms, then word presentation until a response or 2000 ms (whichever was shorter), followed by 500 ms wait time till the next trial. Participants took the Stroop test after a practice run of 2–3 minutes. Each test included 3 blocks of 110 trials and the entire task took about 20 minutes to complete. All participants had accuracy over 76%, indicating alertness. This consistent data collection environment help control all drowsiness, sleepiness, or tiredness and alertness level between the two groups.

2.3. EEG recordings

Online EEG data were collected during the resting state or during the Stroop challenge as previously described(Arakaki et al., 2018). Briefly, a 21-head-sensor, dry electrode system (Quasar Wearable Sensing, DSI-24, San Diego, CA) was used to collect EEG signals. Sensor configuration followed the international 10–20 system. Sensors were placed approximately at the following locations: Fp1, Fp2, F7, F3, Fz, F4, F8, T3, C3, Cz, C4, T4, T5, P3, Pz, P4, T6, O1, O2, M1, and M2, referring to frontal (F), temporal (T), central (C), parietal (P), occipital (O), and mastoidal (M) locations, respectively. EEG signals were sampled at 300 Hz, and bandpass filtered between 0.003–150Hz. To help signal processing, electrooculographic (EOG), electrocardiographic (ECG), and electromyography (EMG) were recorded by three auxiliary sensors. A trigger channel encoded the time of color-word stimuli onset, the participants' responses, and the type of test (C or I) for further analysis.

2.4. Behavioral and EEG Data Processing

The study was double blinded, i.e., the subjects were not aware of group placement and researchers performed all behavioral and EEG data collection and processing without knowledge of CH-NAT/CH-PAT status. Behavioral performances were described and compared by accuracy (ACC) and response time (RT): we define ACC as the percentage of correctly responded trials out of total trials; RT as the duration from stimulus onset to participant's response on correct trials.

We analyzed all datasets in EEGLAB version eeglab14_1_0b(Delorme and Makeig, 2004) running in MATLAB R2016b (The MathWorks, USA) and with custom codes developed in-house. The continuous EEG recordings were segmented into 1500 ms epochs of all correctly responded Stroop trials using the stimulus onset as a reference [−500 1000],

or specific time windows of 1500 ms duration during eyes closed for resting state. Preprocessing and time-frequency analyses were performed as described(Arakaki et al., 2018). Briefly, we filtered epochs between 2 and 30 Hz, re-referenced EEG data to the mean of two mastoid sensors (M1 and M2), and independent component analysis (ICA) (Delorme and Makeig, 2004) was used to remove eye blinks, cardiac, and muscle artifacts. Large artifacts activity higher than three standard deviations (SDs) from a specific sensor's mean were rejected. There were no differences in the number of epochs rejected between CH-NATs (36±17 for congruent trials and 45±25 for incongruent trials) and CH-PATs (35±16 and p=0.85 for congruent trials, 37±17 and p=0.23 for incongruent trials). No channels were labelled bad for either group. For time-frequency analysis, epoched EEG data were decomposed with logarithmic scaling between 2 and 30 Hz by fast Fourier transform and Morlet wavelet [$e^{i2\pi t f} e^{-t^2/2\sigma^2}$] convolution in the frequency domain, followed by the inverse fast Fourier transform(Cohen, 2014; Cohen and Donner, 2013). Power values were normalized by decibels to the baseline power from −400 to −100 ms pre-stimulus at each frequency band [$dB\ power = 10 * \log10(\frac{power}{baseline})$], to sufficiently estimate baseline activity(Cohen, 2017). Based on the TF plots and published data(Hu et al., 2013; Pagano et al., 2015; Vazquez-Marrufo et al., 2017), alpha ERD (mean power in the range 200–500 ms, 8–15 Hz) were then extracted for comparison across sensors, participants, and groups based on the literature(Klimesch, 2012). This was done separately for each sensor, condition, and participant.

Besides alpha ERD, other frequency bands, such as delta, theta, and beta bands, are reported to be essential for Stroop interference processing (Ergen et al., 2014). Therefore, we compared delta (2–4), theta (4–8 Hz), alpha (8–15 Hz), and beta (15–30 Hz) bands at the early [0 to 500] ms window (except alpha at [200 to 500] ms) or late [500 to 1000] ms window between CH-NAT and CH-PAT participants. Alpha SE change from congruent to incongruent trials were also compared.

2.5. Spectral entropy (SE) analysis

We calculated alpha SE for baseline EEG using the [−400 to −100] ms time window during Stroop test trials to avoid early post-stimulus activity influences(Cohen, 2017), and alpha SE for active (ERD) EEG using the [200–500] ms time window. For each time point, we calculated the SE in the respective temporal windows of each EEG channel using the following formula: $SE = \frac{1}{\ln(N)} \sum_{f_i = f_1}^{f_2} P_n(f_i) \ln\left(\frac{1}{P_n(f_i)}\right)$ (Quandt et al., 2016), where N is the number of frequency components in the [f1 f2] range, with f1 and f2 being the lower (8 Hz) and upper (15 Hz) limit of the alpha frequency band respectively, and $P_n(f_i)$ is the normalized power spectrum.

2.6. Cognitive reserve and neuropsychology tests

Verbal IQ was calculated from education, sex, & age norms from our WAIS-III testing. We calculated cognitive reserve from proxies of verbal IQ and education years(Frankenmolen et al., 2018): 1) we calculated Z-scores for verbal IQ and education years for each participant (the difference between individual score and the sample mean score divided by the sample

standard deviation). 2) we averaged the Z-scores of verbal IQ and education years. Mini Mental State Examination and Montreal Cognitive Assessment were measured by standard questionnaire(Crum et al., 1993; Freitas et al., 2013).

2.7. Statistical methods

Alpha power measurements were analyzed by averaging individual sensors within and across participants to derive statistics. We compared group differences in participant baseline characteristics using two-sided t-tests or Fisher's exact tests. We summarized alpha power and alpha SE statistics for 6 regions(Arakaki et al., 2018; Lianyang et al., 2016): frontal or F (Fz, F3, F4), central or C (Cz, C3, C4), parietal or P (Pz, P3, P4), left temporal or LT (F7, T3, T5), right temporal or RT (F8, T4, T6), and occipital or O (O1, O2). We hypothesize that: 1) frontal and/or occipital alpha ERD is more negative in CH-PATs than CH-NATs; 2) frontal and/or occipital alpha SE is higher in CH-PATs than CH-NATs, and frontal and/or occipital alpha SE change from congruent to incongruent trials were lower in CH-PATs compared with CH-NATs. For information, we listed alpha power and SE in all 6 regions.

The strength of associations between frontal alpha ERD/SE with cognitive reserve from the same individuals were assessed as slope factors, determined using linear regression methods and correlation coefficients, and p values were computed. Receiver operating characteristic (ROC) curves were performed to determine whether frontal/occipital alpha ERD or SE alone can classify CH-NAT and CH-PAT participants, and whether multiple logistic regression including alpha ERD or SE with cognitive reserve (main effects only or with two-way interactions) can improve the group classification.

Alpha ERD were compared between CH-NATs and CH-PATs, between A+ and A−T−N− groups, and between a group with any combination of A+ or T+ or N+ biomarker versus a group with all normal biomarkers (A−T−N−).

T-statistic values for comparisons between CH-NATs and CH-PATs were calculated assuming unequal variance and a paired t-test (for Tables S1c&d) was done between congruent and incongruent trials (Kim, 2015). Effect size was calculated using Cohen's d (Rochart et al., 2020). Analyses were done using PRISM v8.4.0 (GraphPad), Excel (Microsoft Office 2013), or MATLAB 2020a. A significance level of 0.05 was used for all tests unless otherwise stated.

3. Results

3.1. Study participant demographics

Cognitively healthy participants with normal Aβ/tau ratios (CH-NAT, n=20), and abnormal Aβ/tau ratios (CH-PAT, n=21), were matched by age, gender, education, and handedness (Table 1). Additional measures were listed including MSD amyloid, p-tau, and total-tau; estimated Innotest amyloid, tau, and amyloid/tau ratio; verbal IQ, cognitive reserve score, and other cardiovascular risk related measures (total cholesterol, HDL, smoke, resting SBP, and resting DBP). No group differences were found. In preliminary re-assessment after 2 years from the time of qEEG/Stroop testing, 3 of the CH-PAT group and none of the CH-NAT group have declined.

3.2. Behavioral Performance (ACC and RT)

For the congruent and incongruent trials, neither ACC nor RT was significantly different between the CH-NAT and CH-PAT participants (Table 2). RT during incongruent trials was longer than that during congruent trials for both groups ($p<0.001$). Accuracy during incongruent trials was lower than that during congruent trials for both CH-NATs and CH-PATs ($p<0.01$).

3.3. Alpha during resting state and alpha during task baseline values

We compared CH-NAT and CH-PAT participants on time-frequency plots for mean alpha power during resting, and during congruent and incongruent trial baselines. Our analyses suggest that alpha power is comparable between the two groups, during eyes open resting (Frontal: −0.79±1.20 for CH-NATs and −0.32±1.18 for CH-PATs, p=0.214; Occipital: −0.68±1.47 for CH-NATs and −0.22±0.65 for CH-PATs, p=0.200), during eyes closed (Frontal: −0.73±0.69 for CH-NATs and −0.77±1.29 for CH-PATs, p=0.908; Occipital: −0.69±1.18 for CH-NATs and −0.77±1.36 for CH-PATs, p=0.830), and baseline of congruent and incongruent trials (was used for normalization).

3.4. Time-Frequency Plots and Alpha ERD differences during cognitive challenge

Figure 1 shows the fronto-posterior distribution of alpha ERD during the Stroop test, comparing CH-NAT versus CH-PAT, assessing the time-frequency plots of mean power of EEG in the sagittal plane in the frontal, central, parietal, and occipital regions of the brain. Despite comparable behavioral performance measures (Table 2), the total power of alpha ERD, in the white box in the occipital region (congruent trials), was significantly decreased (more negative, blue color) (200~500 ms, 8–15 Hz) in the CH-PAT group compared to age-matched CH-NATs, indicated by the arrows in Figure 1.

During congruent trials, occipital alpha ERD was lower in CH-PAT than CH-NAT (df=38, t=2.35, p=0.024) (Fig 2, Table 3a). During incongruent trials, frontal and occipital alpha ERD was not different between CH-NATs and CH-PATs (Frontal: p=0.423, Occipital: p=0.193) (Fig 2 and Table 3b). Compare alpha ERD changes from congruent to incongruent trials, CH-PATs presented lower occipital alpha ERD changes than CH-PATs (df=34, t=2.68, p=0.011) (Figure 2, Table 3c).

When comparing the normal CSF group (A−T−N−) (n=19) to the group with the most widely accepted AD biomarker (A+) (n=12), alpha ERD was not different among any of the regions during congruent trials, incongruent trials, or changes from congruent to incongruent trials (Tables 4a–c). When comparing alpha ERD between the A−T−N− group (n=19) versus the A+ or T+ or N+ group (n=22), no different alpha ERD was observed (Data not shown).

3.5. Frontal/occipital alpha SE differences during cognitive challenge

During congruent trials, CH-PATs presented higher alpha SE (active ERD windows) compared to CH-NATs (Frontal: df=38, t=−2.49, p=0.017 and Occipital: df=38, t=−2.43, p=0.020). There were no frontal or occipital alpha SE differences between the two groups during incongruent trials (Fig 3 and Table 5). Comparing alpha SE changes from congruent

to incongruent trials, CH-PATs presented lower frontal alpha SE changes than CH-NATs (df=27, t=2.55, p=0.012) (Fig 3, right column; Table 5c).

3.6. Frontal/Occipital Alpha ERD, SE and cognitive reserve correlation by groups

Alpha ERD correlated positively with cognitive reserve during incongruent trials in the frontal (r=0.66, p=0.001) and occipital (r=0.55, p=0.009) regions for CH-PATs, but not for CH-NATs. Neither group shows correlations during congruent trials (Fig 4). Cognitive reserve correlated negatively with alpha SE during incongruent trials at frontal (r=−0.57, p=0.007) and occipital (r=−0.47, p=0.033) regions for CH-PATs, but not CH-NATs. Neither group shows correlations between alpha SE and cognitive reserve during congruent trials (Fig 4E–H).

3.7. Receiver operating characteristic (ROC) curves

We examined whether frontal and occipital alpha ERD or SE, and cognitive reserve distinguished CH-PATs from CH-NATs. The overlap ROC curves show frontal alpha ERD during congruent trials (Fc, AUC=0.58, p=0.389), occipital alpha ERD during congruent trials (Oc, AUC=0.69, p=0.039), cognitive reserve (AUC=0.56,p=0.514), Montreal Cognitive Assessment (MoCA: AUC=0.63, p=0.167), and Mini Mental State Examination (MMSE: AUC=0.61, p=0.241) were different classifiers. The combinations of frontal/occipital alpha ERD (Fc, Oc) and cognitive reserve improved the prediction of CH-PATs (AUC=0.72, p=0.014). Further considering the two-way interactions, the combinations of frontal/occipital alpha ERD (Fc, Oc) and cognitive reserve were significant classifiers of CH-NATs and CH-PATs (AUC=0.81, p=0.0006). However, incongruent frontal alpha ERD (Fi, AUC=0.54, p=0.649), occipital alpha ERD (Oi, AUC=0.60, p=0.297) were not significant. Combinations of incongruent alpha ERD (Fi, Oi) and cognitive reserve were significant binary classifiers of CH-NATs/CH-PATs (AUC=0.65, p=0.110), which were more significant when considering two-way interactions (AUC=0.75, p=0.008).

For alpha SE, overlap ROC curves show congruent alpha SE at frontal (Fc, AUC=0.73, p=0.012), occipital (Oc, AUC=0.69, p=0.035) regions, cognitive reserve (AUC=0.56,p=0.514), Montreal Cognitive Assessment (AUC=0.63, p=0.167), and Mini Mental State Examination (AUC=0.61, p=0.241) were different classifiers for CH-NATs and CH-PATs. The combination of frontal and occipital alpha ERD during congruent trials (Fc, Oc) and cognitive reserve improved the prediction of CH-PATs (AUC=0.75, p=0.005), which were more significant when considering two-way interactions (AUC=0.83, p=0.0003). However, the congruent to incongruent alpha SE changes at frontal (Fci, AUC=0.72, p=0.020), occipital (Oci, AUC=0.58, p=0.403) regions were different classifiers. The combinations of congruent to incongruent changes of alpha SE (Fci, Oci) and cognitive reserve improved the prediction of CH-PATs (AUC=0.72, p=0.021), which were more significant when considering two-way interactions (AUC=0.81, p=0.0001) (Figure 5).

3.8. Other frequency band by groups

Delta, theta, alpha, and beta power at early (before 500ms) and late (500–1000ms) window during Stroop testing were compared. Table S1 shows some differences besides the aforementioned alpha ERD domain. During congruent trials, late delta power at the

occipital region was also lower in CH-PATs than CH-NATs (p = 0.017) (Table S1a); During incongruent trials, late theta power was lower in CH-PATs than CH-NATs (p = 0.013 for right temporal and 0.048 for occipital region) (Table S1b). Compared to that during congruent trials, CH-NATs had higher centroparietal theta during incongruent trials, while CH-PATs had more negative temporo-occipital alpha and beta in addition to higher parietal theta (Tables S1c&1d).

3.9. Spectral power correlate with Response time by groups

The correlation between participants' spectral power and RT for different trials were shown in topoplots (n=17 for CH-NATs and n=21 for CH-PATs). During congruent trials, CH-PATs beta power positively correlated with RT (p=0.006~0.048, r=0.44~0.58, at frontocentroparietal regions); CH-NATs theta power negatively correlated with RT (p=0.006~0.033, r=−0.63 ~ −0.52, at frontocentroparietal regions); Both groups' delta negatively correlated with RT, with CH-NATs limited at centroparietal regions (p=0.003~0.016, r=−0.67~ −0.58) and CH-PATs at all regions (p=0.001~ 0.017, r=−0.68~ −0.51). Similarly, during incongruent trials for delta power, both groups correlate negatively with RT, with CH-NATs limited at frontocentroparietal regions (p=0.003~0.022, r=−0.68~ −0.55), while CH-PATs have all except left temporal regions (0.004~0.039, r=−0.60~ −0.45) (Figure 5B). Details and correlations with ACC are shown in supplement (Tables S2).

3.10. Spectral power correlates with CSF amyloid, total Tau, Mini Mental State Examination, and amyloid/tau ratio

The participants' EEG spectral powers were correlated with CSF amyloid, total Tau, and Mini Mental State Examination (n=17 for CH-NATs and n=21 for CH-PATs). Briefly, for CSF amyloid level during congruent trails, CH-NATs' delta correlated positively with amyloid (p=0.013~0.042, r=0.50~0.59 for Parietal, Right temporal regions). During incongruent trials, CH-NATs' delta correlated positively with amyloid (p=0.002~0.043, r=0.50~0.69 for Frontocentroparietal regions). For CSF tau level during congruent trials, CH-PATs' alpha correlated with Tau (p=0.016~0.047, r=0.44~0.52 in Frontocentral and Left temporal regions), CH-NATs' delta correlated with Tau (p=0.004~0.024, r=0.45~0.59, F, P, RT regions); during incongruent trials, CH-NATs' delta correlated with Tau (p=0.004, r=0.65~0.67 for Parietal and Right temporal regions). Details in Tables S3a&b). For Mini Mental State Examination during congruent trials, CH-NATs' beta correlated negatively with Mini Mental State Examination (p=0.028~0.039, r=−0.53~−0.50 for Centroparieto-occipital regions); during incongruent trials, CH-NATs' beta correlated negatively with Mini Mental State Examination over all regions (p=0.006~0.043, r=−0.64~−0.50). Tables S3a&b show details. We listed the relationships between alpha ERD or SE with CSF amyloid/Tau ratios across all cognitively healthy individuals, and within each group (Table S4).

4. Discussion

Our study demonstrates that the Stroop challenge reveals subtle changes in CH-PATs compared to CH-NATs and supports our two predictions: First, despite similar behavioral responses, occipital alpha ERD was decreased (more negative) and frontal and occipital alpha SE were higher in CH-PATs during a low interference load, indicating hyperactivity;

frontal alpha SE changes from low to high interference load were lower in CH-PATs, suggesting insufficient cognitive resources with increasing interference load. The different qEEG between CH-NAT and CH-PAT groups during Stroop testing highlights the importance of the qEEG data in revealing underlying susceptibility for individuals with pathological CSF amyloid/tau. We emphasize the accuracy and generalizability of our qEEG in this paradigm, since the RTs (600~1000 ms) of our participants are consistent with the reported range for computerized Stroop testing(Tse et al., 2010), and both groups exhibited the expected Stroop effects with longer RT during incongruent than congruent trials. Second, there are significant correlations between alpha ERD with cognitive reserve in CH-PATs compared to CH-NATs. These qEEG measures during a simple cognitive "interference" challenge were linked to cognitive reserve, suggesting that the cognitive resistances (proxies of education and verbal IQ) to early amyloid/tau abnormalities are related to compromised interference processing in CH-PATs.

Our participants CH-PATs had higher CSF total tau than that in CH-NATs, while amyloid levels are comparable between two groups. The amyloid and tau status suggest our population likely included individuals with non-Alzheimer's pathology, or suspected non-Alzheimer's pathophysiology (SNAP): A−T+(N)−, A−T−(N)+, or A−T+(N)+(Jack et al., 2018). CSF measures have been reported to be more sensitive than imaging measures(Lee et al., 2020). In this study, differences in alpha ERD were observed between groups based on amyloid/tau ratio, but not between A−T−N− and A+ (AD biomarker) groups or between A−T−N− and any combination of the A+ or T+ or N+ group. This is consistent with previous studies about amyloid/tau ratio advantages. For example, the amyloid/tau ratio outperforms any individual protein in discriminating those with cortical amyloid(Fagan et al., 2011), and thus should be a more sensitive predictor of AD risk than total tau alone(Roe et al., 2013). Studies have also demonstrated the CSF tau (t- or p-Tau)/Abeta ratio's capacity to predict MCI progression to AD(Ritchie et al., 2017). The ratio of CH individuals with AD-biomarker among CH with A+ (12 out of 22, or ~55%) is a bit lower than that in the CH group from a previous ATN biomarker study (39% out of 58%, or ~67%) (Ekman et al., 2018), but still covers over half of the individual biomarker population. In addition to the ATN research framework (Jack et al., 2018), there are some interesting facts. Firstly, the most common dementia type is AD and pathological heterogeneity is extensive in sporadic, late-onset AD (Schneider et al., 2009). Secondly, there are reports of tau or neurodegeneration biomarkers changing first in preclinical AD and in AD pathology(Dubois et al., 2016; Jack and Holtzman, 2013; Jack et al., 2013). As AD is the dominant etiology among all dementia types, we focus our discussion on AD in this study. Ongoing longitudinal follow up of the clinical, CSF biomarkers and the amyloid/tau ratio, and qEEG in our population will help to interpret the alpha ERD relationship to combinations of these and other biomarkers.

4.1. The yield of interference challenge

We focused on frontal and occipital alpha ERD and alpha SE in this study based on previous publications. Firstly, abnormal frontal/occipital alpha were reported during the resting state: Nakamura et al. reported local amyloid-beta deposition related frontal alpha band augmentation in preclinical AD(Nakamura et al., 2018), Qi's group has reported

increased frontal activity in amnestic MCI using fMRI(Qi et al., 2010). Babiloni's group has reported that occipital alpha current density decreased in MCI and AD participants than healthy elderlies and occipital alpha activity related to local gray matter density in all participants(CH, MCI, AD)(Babiloni et al., 2015). Secondly, Nombela et al. reported reduced frontal and occipital alpha with age (the main risk factor for AD) during Stroop testing(Nombela et al., 2014). Lastly, our previous pilot study, and others, supported frontal hyperactivity (more negative alpha ERD and higher alpha SE) in CH-PATs during working memory testing, a core executive function related to Stroop interference (Arakaki et al., 2019; Harrington et al., 2013; Jaiswal et al., 2019; Rochart et al., 2020).

Our study is novel because it uses both an early stage of amyloid/tau pathology detectable only by CSF biomarkers, and cognitive challenge (interference) to reveal alterations in dynamic neural responses detected by both qEEG and by its link to cognitive reserve. We have listed alpha ERD's potential interactions with other AD related measures (Mini Mental State Examination, and CSF amyloid/tau) in the Supplementary Tables S3&4 in order to stimulate future interests of these new qEEG related findings and potential AD pathophysiology.

4.2. Context of Previous Work and relation to prior EEG and MEG-based biomarkers

Several studies reported impaired Stroop performance with AD risk, including: higher Stroop reaction time variations in preclinical AD or early AD(Patten et al., 2018; Tse et al., 2010), reduced interference and goal maintenance in MCI and further reduction in AD(Belanger et al., 2010). We did not find behavioral performance changes in Stroop, probably due to different study group (cognitively healthy vs. early AD or MCI).

Resting EEG studies report alpha changes in AD. In the symptomatic stage, alpha in MCI and AD patients changes mostly at the frontal and occipital regions: Bajo et al. reported higher parieto-occipital synchronization in alpha and beta bands for progressive MCI compared to stable MCI(Bajo et al., 2012); Babiloni's group reported reduced frontal and occipital alpha and alpha connectivity in AD than healthy elderly participants(Babiloni et al., 2016); AD patients presented occipital hypo-synchronous alpha by resting MEG than age-match controls, and the hypo-synchronous alpha in AD related to decreased Mini Mental State Examination score and co-localized with local tau deposition(Ranasinghe et al., 2020); and preclinical AD individuals demonstrate frontal hyperactivity(Nakamura et al., 2018). We did not see resting frontal or occipital alpha changes, possibly due to the early disease stage (amyloid/tau pathology detected by CSF earlier than by brain imaging) or different techniques (low-density EEG vs. high-density MEG).

For EEG during Stroop, Jiang et al. reported semantic and response conflict revealed frontal theta modulation and occipito-parietal alpha reduction, in undergraduate students aged 19–24(Jiang et al., 2015). Older adults presented decreased alpha and theta activity during epochs related to mind-wandering (after errors)(Atchley et al., 2017). Older participants (60's) show decreased frontal and occipital alpha during Stroop than younger ones(Nombela et al., 2014). Different reports in the literatures could be partly attributable to different methods (e.g., different workload or alpha measurements). For example, alpha activity (e.g., event-related synchronization, ERS) has been linked to inhibitory gating in task-irrelevant

areas(Jensen and Mazaheri, 2010; Klimesch, 2012; Klimesch et al., 2007), and alpha ERD responses were considered as a functional correlate of brain activation(Klimesch, 2012; Klimesch et al., 2007). We interpret our finding of more negative alpha ERD in the occipital region with higher alpha SE over the frontal and occipital regions during congruent trials as supporting compensatory hyperactivity in CH-PATs. This result corroborates our previous findings of higher frontal alpha SE during low load working memory testing(Arakaki et al., 2019). An interesting connection is that working memory capacity can predict the Stroop interference level(Kane and Engle, 2003; Tse et al., 2010). Our data during the low load interference challenge supports our hypothesis that CH-PATs present more negative alpha ERD in the occipital region and higher alpha SE over the frontal and occipital regions. This frontal and occipital hyperactivity seems to be transitional for lower long-distant connections seen in AD participants(Stam et al., 2009). Additionally, we interpret the lower alpha SE from congruent to incongruent trials in the frontal region in CH-PATs to suggest insufficient cognitive recruitment in response to higher load challenge.

Alpha ERD was induced at different frequency ranges: 8–13 Hz from nociceptive stimuli (Hu et al., 2013), 10–14 Hz during a visual oddball cognitive task (Vazquez-Marrufo et al., 2017), 8–15 Hz during an enumeration task (Pagano et al., 2015), and 8–12 Hz during memory task (Krause et al., 2008). Interestingly, the 12–15 Hz range has been studied during nonrapid eye movement sleep as sigma activity or “sleep spindles” (Riedner et al., 2016), during encephalopathy as “coma spindles” (Bortone et al., 1996; Dadmehr et al., 1987), or part of low beta. We used 8–15 Hz for alpha frequency range as previously studied (Arakaki et al., 2019; Pagano et al., 2015).

Besides alpha, frontal theta has been related to conflict responses(Atchley et al., 2017; Jiang et al., 2015; Nombela et al., 2014; Xavier et al., 2020). We observed higher centroparietal theta during incongruent trials than congruent trials in CH-NATs (Supplementary Tables S1c&d). These are not discussed further as they are beyond the scope of this study.

4.3. Cognitive reserve and alpha ERD are correlated in CH-PATs

Structural and functional changes are known to precede cognitive decline in AD progression, and there are inter-individual differences in cognitive symptomatic delay(Menardi et al., 2018). Cognitive reserve has been used to account for cognitive performance variabilities: cognitive reserve reflects an individual’s ability to preserve cognitive function from aging or neurodegenerative pathology in the early stage(Stern, 2009), however after AD diagnosis, individuals with higher cognitive reserve deteriorate faster(Wilson et al., 2000). Higher cognitive reserve is associated with more effective strategies in executive tasks(Barulli et al., 2013; Frankenmolen et al., 2018) and with lower levels of cardiovascular disease (white matter hyperintensities), which may offer resilience to other pathologies(Pettigrew et al., 2020). Higher cognitive reserve has been related to resilience to cognitive decline from white matter lesions(Giogkaraki et al., 2013; Mortamais et al., 2014) and greater resting-state lagged linear connectivity as a measure of inter-regional connectivity(Fleck et al., 2019). To our knowledge, no other studies correlate cognitive reserve with alpha ERD.

Cognitive reserve can be estimated by proxies of education years and verbal IQ(Frankenmolen et al., 2018; Narbutas et al., 2019). We interpret the alpha ERD correlation

with cognitive reserve in CH-PATs during incongruent trials to indicate a strain on cognitive reserve by the high load interference challenge. Interestingly, CH-PATs with higher cognitive reserve have increased alpha ERD values (less negative), indicating a better neural efficiency that more resembles the findings in CH-NATs. Although spectral entropy is not different between the two groups during incongruent trials, the correlation with cognitive reserve is only significant (negatively) in CH-PATs: CH-PAT participants with higher cognitive reserve used less alpha SE for high load incongruent trials, suggesting higher neural efficiency with fewer resources used for the task. These results are consistent with our interpretation of the alpha ERD results. Therefore, our data support the idea that cognitive reserve may protect neural function (higher ERD and lower SE) from pathological CSF amyloid/tau levels, in line with the protective role of education(Gatz, 2005). Our study also echoed study of resting state occipital/temporal alpha interaction with education attainment in a preclinical AD population (amyloid PET-positive subjective memory complaint seniors) (Babiloni et al., 2020b). The different neuroprotective alpha 2 and compensatory alpha 3 effects in Babiloni's study are beyond our focus here but are worth exploring further. We used the common cognitive reserve calculation from verbal IQ and years of education; adding factors such as occupational complexity, physical activity, leisure activities, etc., may further improve this type of analysis(Narbutas et al., 2019).

The cognitive reserve and alpha ERD/SE correlation in CH-PATs is significant during incongruent trials, suggesting their interference processing during high load Stroop challenge depends on the protective effects of cognitive reserve. On the other hand, cognitive reserve is not different when directly compared between the two groups, suggesting that compromised interference processing in CH-PATs does not result from different cognitive reserve directly. This relationship is worth further study at different AD stages.

In summary, our pilot study supports compensatory hyperactivity in CH-PATs during low load interference challenge and insufficient brain resources with higher workload compared with CH-NATs.

4.4. Limitations, clinical implications, and future studies

There are limitations to this study. First, the investigation was exploratory, and participants from the local Pasadena area were mainly Caucasian with higher socioeconomic status. This work needs to be repeated in a larger, more diverse population. With longitudinal follow up, potential biomarkers can be calculated to set standards for clinical screening. In addition, Stroop interference does not include typical conflicts in real life (e.g., left vs. right). Future studies could incorporate different interference factors, such as the Simon effect (Ma and Shang, 2013). Finally, more participants are female than male, both for CH-NATs and CH-PATs, which may reflect either greater altruism in participation, or greater resilience to aging in females. Our results regarding alpha ERD and alpha SE during Stroop task performance provide new insight into early amyloid/tau pathology and encourage further research.

5. Conclusions

Stroop testing combined with qEEG in a cross-sectional study revealed that interference processing is compromised in cognitively healthy individuals with AD biomarkers defined by CSF pathological amyloid/tau ratio. Our results show that alpha ERD correlates with cognitive reserve in individuals with CH-PAT biomarkers. We demonstrate for the first time that insufficient brain resources in CH-PAT individuals are revealed by interference Stroop testing and are probably a transitional stage to further deterioration. We propose that treatment strategies to improve cognitive reserve at the pre-symptomatic stage of AD may help resist neurodegeneration(Suffczynski et al., 2001). Cognitive challenge with Stroop testing combined with qEEG have valuable screening potential to differentiate CH-PAT from CH-NATs and offer useful tools to monitor and guide new therapies.

Supplementary Material

Refer to Web version on PubMed Central for supplementary material.

Acknowledgments

We thank the study participants for their contributions. Betty Chung and David Buennagel assisted with participant recruitment and faculty-supervised graduate students of Fuller psychology department performed psychometry testing. Dr. Quanying Liu helped with the estimated Innotest amyloid and tau conversions. Some data relied upon in this study was derived from research performed at HMRI by Dr. Michael G. Harrington.

Funding

This work was supported by the National Institutes of Aging [grant number R56AG063857, R01AG063857] and L. K. Whittier Foundation.

Abbreviations:

AD	Alzheimer’s disease
CH-NATs	cognitively healthy with normal CSF amyloid/tau ratio
CH-PATs	cognitively healthy with pathological CSF amyloid/tau ratio
EEG	electroencephalography
ERD	event-related desynchronization
SE	spectral entropy

References

Arakaki X, Lee R, King KS, Fonteh AN, Harrington MG, 2019. Alpha desynchronization during simple working memory unmasks pathological aging in cognitively healthy individuals. PLoS One 14(1), e0208517. [PubMed: 30601822]

Arakaki X, Shoga M, Li L, Zouridakis G, Tran T, Fonteh AN, Dawlaty J, Goldweber R, Pogoda JM, Harrington MG, 2018. Alpha desynchronization/synchronization during working memory testing is compromised in acute mild traumatic brain injury (mTBI). PLoS One 13(2), e0188101. [PubMed: 29444081]

Atchley R, Klee D, Oken B, 2017. EEG Frequency Changes Prior to Making Errors in an Easy Stroop Task. Front Hum Neurosci 11, 521. [PubMed: 29163101]

Babiloni C, Blinowska K, Bonanni L, Cichocki A, De Haan W, Del Percio C, Dubois B, Escudero J, Fernandez A, Frisoni G, Guntekin B, Hajos M, Hampel H, Ifeachor E, Kilborn K, Kumar S, Johnsen K, Johannsson M, Jeong J, LeBeau F, Lizio R, Lopes da Silva F, Maestu F, McGeown WJ, McKeith I, Moretti DV, Nobili F, Olichney J, Onofrj M, Palop JJ, Rowan M, Stocchi F, Struzik ZM, Tanila H, Teipel S, Taylor JP, Weiergraber M, Yener G, Young-Pearse T, Drinkenburg WH, Randall F, 2020a. What electrophysiology tells us about Alzheimer's disease: a window into the synchronization and connectivity of brain neurons. Neurobiol Aging 85, 58–73. [PubMed: 31739167]

Babiloni C, Del Percio C, Boccardi M, Lizio R, Lopez S, Carducci F, Marzano N, Soricelli A, Ferri R, Triggiani AI, Prestia A, Salinari S, Rasser PE, Basar E, Fama F, Nobili F, Yener G, Emek-Savas DD, Gesualdo L, Mundi C, Thompson PM, Rossini PM, Frisoni GB, 2015. Occipital sources of resting-state alpha rhythms are related to local gray matter density in subjects with amnesic mild cognitive impairment and Alzheimer's disease. Neurobiol Aging 36(2), 556–570. [PubMed: 25442118]

Babiloni C, Lopez S, Del Percio C, Noce G, Pascarelli MT, Lizio R, Teipel SJ, Gonzalez-Escamilla G, Bakardjian H, George N, Cavedo E, Lista S, Chiesa PA, Vergallo A, Lemercier P, Spinelli G, Grothe MJ, Potier MC, Stocchi F, Ferri R, Habert MO, Fraga FJ, Dubois B, Hampel H, Group I.N.-p.S., 2020b. Resting-state posterior alpha rhythms are abnormal in subjective memory complaint seniors with preclinical Alzheimer's neuropathology and high education level: the INSIGHT-preAD study. Neurobiol Aging 90, 43–59. [PubMed: 32111391]

Babiloni C, Triggiani AI, Lizio R, Cordone S, Tattoli G, Bevilacqua V, Soricelli A, Ferri R, Nobili F, Gesualdo L, Millan-Calenti JC, Bujan A, Tortelli R, Cardinali V, Barulli MR, Giannini A, Spagnolo P, Armenise S, Buenza G, Scianatico G, Logroscino G, Frisoni GB, Del Percio C, 2016. Classification of Single Normal and Alzheimer's Disease Individuals from Cortical Sources of Resting State EEG Rhythms. Front Neurosci 10, 47. [PubMed: 26941594]

Bajo R, Castellanos NP, Cuesta P, Aurtenetxe S, Garcia-Prieto J, Gil-Gregorio P, del-Pozo F, Maestu F, 2012. Differential patterns of connectivity in progressive mild cognitive impairment. Brain Connect 2(1), 21–24. [PubMed: 22458376]

Barulli DJ, Rakitin BC, Lemaire P, Stern Y, 2013. The influence of cognitive reserve on strategy selection in normal aging. J Int Neuropsychol Soc 19(7), 841–844. [PubMed: 23714237]

Bateman RJ, Wen G, Morris JC, Holtzman DM, 2007. Fluctuations of CSF amyloid-beta levels: implications for a diagnostic and therapeutic biomarker. Neurology 68(9), 666–669. [PubMed: 17325273]

Belanger S, Belleville S, Gauthier S, 2010. Inhibition impairments in Alzheimer's disease, mild cognitive impairment and healthy aging: effect of congruency proportion in a Stroop task. Neuropsychologia 48(2), 581–590. [PubMed: 19879885]

Bortone E, Bettoni L, Buzio S, Delsoldato S, Giorgi C, Mancia D, 1996. Spindle coma and alternating pattern in the course of measles encephalitis. Clin Electroencephalogr 27(4), 210–214. [PubMed: 9465285]

Cohen MX, 2014. Analyzing Neural Time Series Data: Theory and Practice.

Cohen MX, 2017. Rigor and replication in time-frequency analyses of cognitive electrophysiology data. Int J Psychophysiol 111, 80–87. [PubMed: 26876335]

Cohen MX, Donner TH, 2013. Midfrontal conflict-related theta-band power reflects neural oscillations that predict behavior. J Neurophysiol 110(12), 2752–2763. [PubMed: 24068756]

Crum RM, Anthony JC, Bassett SS, Folstein MF, 1993. Population-based norms for the Mini-Mental State Examination by age and educational level. JAMA 269(18), 2386–2391. [PubMed: 8479064]

Cummings J, Lee G, Ritter A, Sabbagh M, Zhong K, 2019. Alzheimer's disease drug development pipeline: 2019. Alzheimers Dement (N Y) 5, 272–293. [PubMed: 31334330]

Dadmehr N, Pakalnis A, Drake ME Jr., 1987. Spindle coma in viral encephalitis. Clin Electroencephalogr 18(1), 34–37. [PubMed: 3829433]

Delorme A, Makeig S, 2004. EEGLAB: an open source toolbox for analysis of single-trial EEG dynamics including independent component analysis. J Neurosci Methods 134(1), 9–21. [PubMed: 15102499]

Dubois B, Hampel H, Feldman HH, Scheltens P, Aisen P, Andrieu S, Bakardjian H, Benali H, Bertram L, Blennow K, Broich K, Cavedo E, Crutch S, Dartigues JF, Duyckaerts C, Epelbaum S, Frisoni GB, Gauthier S, Genthon R, Gouw AA, Habert MO, Holtzman DM, Kivipelto M, Lista S, Molinuevo JL, O'Bryant SE, Rabinovici GD, Rowe C, Salloway S, Schneider LS, Sperling R, Teichmann M, Carrillo MC, Cummings J, Jack CR Jr., Proceedings of the Meeting of the International Working, G., the American Alzheimer's Association on "The Preclinical State of, A.D., July, Washington Dc, U.S.A., 2016. Preclinical Alzheimer's disease: Definition, natural history, and diagnostic criteria. Alzheimers Dement 12(3), 292–323. [PubMed: 27012484]

Ekman U, Ferreira D, Westman E, 2018. The A/T/N biomarker scheme and patterns of brain atrophy assessed in mild cognitive impairment. Sci Rep 8(1), 8431. [PubMed: 29849029]

Ergen M, Saban S, Kirmizi-Alsan E, Uslu A, Keskin-Ergen Y, Demiralp T, 2014. Time-frequency analysis of the event-related potentials associated with the Stroop test. Int J Psychophysiol 94(3), 463–472. [PubMed: 25135670]

Fagan AM, Shaw LM, Xiong C, Vanderstichele H, Mintun MA, Trojanowski JQ, Coart E, Morris JC, Holtzman DM, 2011. Comparison of analytical platforms for cerebrospinal fluid measures of beta-amyloid 1–42, total tau, and p-tau181 for identifying Alzheimer disease amyloid plaque pathology. Arch Neurol 68(9), 1137–1144. [PubMed: 21555603]

Fleck JI, Arnold M, Dykstra B, Casario K, Douglas E, Morris O, 2019. Distinct Functional Connectivity Patterns Are Associated With Social and Cognitive Lifestyle Factors: Pathways to Cognitive Reserve. Front Aging Neurosci 11, 310. [PubMed: 31798441]

Frankenmolen NL, Fasotti L, Kessels RPC, Oosterman JM, 2018. The influence of cognitive reserve and age on the use of memory strategies. Exp Aging Res 44(2), 117–134. [PubMed: 29308968]

Freitas S, Simoes MR, Alves L, Santana I, 2013. Montreal cognitive assessment: validation study for mild cognitive impairment and Alzheimer disease. Alzheimer Dis Assoc Disord 27(1), 37–43. [PubMed: 22193353]

Gatz M, 2005. Educating the brain to avoid dementia: can mental exercise prevent Alzheimer disease? PLoS Med 2(1), e7. [PubMed: 15696217]

Giogkaraki E, Michaelides MP, Constantinidou F, 2013. The role of cognitive reserve in cognitive aging: results from the neurocognitive study on aging. J Clin Exp Neuropsychol 35(10), 1024–1035. [PubMed: 24134146]

Harari O, Cruchaga C, Kauwe JS, Ainscough BJ, Bales K, Pickering EH, Bertelsen S, Fagan AM, Holtzman DM, Morris JC, Goate AM, Alzheimer's Disease Neuroimaging I, 2014. Phosphorylated tau-Abeta42 ratio as a continuous trait for biomarker discovery for early-stage Alzheimer's disease in multiplex immunoassay panels of cerebrospinal fluid. Biol Psychiatry 75(9), 723–731. [PubMed: 24548642]

Harrington MG, Chiang J, Pogoda JM, Gomez M, Thomas K, Marion SD, Miller KJ, Siddarth P, Yi X, Zhou F, Lee S, Arakaki X, Cowan RP, Tran T, Charleswell C, Ross BD, Fonteh AN, 2013. Executive function changes before memory in preclinical Alzheimer's pathology: a prospective, cross-sectional, case control study. PLoS One 8(11), e79378. [PubMed: 24260210]

Harrington MG, Edminster SP, Buennagel DP, Chiang JP, Sweeney MD, CHui HC, V ZB, Fonteh AN, 2019. Four-Year Longitudinal Study of Cognitively Healthy Individuals: CSF Amyloid/Tau Levels and Nanoparticle Membranes Identify High Risk For Alzheimer's Disease. Alzheimer's & Dementia 15(7S).

Hu L, Peng W, Valentini E, Zhang Z, Hu Y, 2013. Functional features of nociceptive-induced suppression of alpha band electroencephalographic oscillations. J Pain 14(1), 89–99. [PubMed: 23273836]

Inouye T, Shinosaki K, Sakamoto H, Toi S, Ukai S, Iyama A, Katsuda Y, Hirano M, 1991. Quantification of EEG irregularity by use of the entropy of the power spectrum. Electroencephalogr Clin Neurophysiol 79(3), 204–210. [PubMed: 1714811]

Jack CR Jr., Bennett DA, Blennow K, Carrillo MC, Dunn B, Haeberlein SB, Holtzman DM, Jagust W, Jessen F, Karlawish J, Liu E, Molinuevo JL, Montine T, Phelps C, Rankin KP, Rowe CC, Scheltens P, Siemers E, Snyder HM, Sperling R, Contributors, 2018. NIA-AA Research Framework: Toward

a biological definition of Alzheimer's disease. Alzheimers Dement 14(4), 535–562. [PubMed: 29653606]

Jack CR Jr., Holtzman DM, 2013. Biomarker modeling of Alzheimer's disease. Neuron 80(6), 1347–1358. [PubMed: 24360540]

Jack CR Jr., Wiste HJ, Weigand SD, Knopman DS, Lowe V, Vemuri P, Mielke MM, Jones DT, Senjem ML, Gunter JL, Gregg BE, Pankratz VS, Petersen RC, 2013. Amyloid-first and neurodegeneration-first profiles characterize incident amyloid PET positivity. Neurology 81(20), 1732–1740. [PubMed: 24132377]

Jaiswal S, Tsai SY, Juan CH, Muggleton NG, Liang WK, 2019. Low delta and high alpha power are associated with better conflict control and working memory in high mindfulness, low anxiety individuals. Soc Cogn Affect Neurosci 14(6), 645–655. [PubMed: 31119291]

Jensen O, Mazaheri A, 2010. Shaping functional architecture by oscillatory alpha activity: gating by inhibition. Front Hum Neurosci 4, 186. [PubMed: 21119777]

Jiang J, Zhang Q, Van Gaal S, 2015. EEG neural oscillatory dynamics reveal semantic and response conflict at difference levels of conflict awareness. Sci Rep 5, 12008. [PubMed: 26169473]

Kane MJ, Engle RW, 2003. Working-memory capacity and the control of attention: the contributions of goal neglect, response competition, and task set to Stroop interference. J Exp Psychol Gen 132(1), 47–70. [PubMed: 12656297]

Kim TK, 2015. T test as a parametric statistic. Korean J Anesthesiol 68(6), 540–546. [PubMed: 26634076]

Klimesch W, 2012. alpha-band oscillations, attention, and controlled access to stored information. Trends Cogn Sci 16(12), 606–617. [PubMed: 23141428]

Klimesch W, Sauseng P, Hanslmayr S, 2007. EEG alpha oscillations: the inhibition-timing hypothesis. Brain Res Rev 53(1), 63–88. [PubMed: 16887192]

Krause CM, Boman PA, Sillanmaki L, Varho T, Holopainen IE, 2008. Brain oscillatory EEG event-related desynchronization (ERD) and -sychronization (ERS) responses during an auditory memory task are altered in children with epilepsy. Seizure 17(1), 1–10. [PubMed: 17588781]

Larson MJ, Kaufman DA, Perlstein WM, 2009. Conflict adaptation and cognitive control adjustments following traumatic brain injury. J Int Neuropsychol Soc 15(6), 927–937. [PubMed: 19765356]

Lee J, Jang H, Kang SH, Kim J, Kim JS, Kim JP, Kim HJ, Seo SW, Na DL, 2020. Cerebrospinal Fluid Biomarkers for the Diagnosis and Classification of Alzheimer's Disease Spectrum. J Korean Med Sci 35(44), e361. [PubMed: 33200589]

Li C, Zheng J, Wang J, Gui L, Li C, 2009. An fMRI stroop task study of prefrontal cortical function in normal aging, mild cognitive impairment, and Alzheimer's disease. Curr Alzheimer Res 6(6), 525–530. [PubMed: 19747163]

Lianyang L, Arakaki X, Thao T, Harrington M, Padhye N, Zouridakis G, 2016. Brain activation profiles in mTBI: evidence from ERP activity of working memory response. Conf Proc IEEE Eng Med Biol Soc 2016, 1862–1865.

Ma Q, Shang Q, 2013. The influence of negative emotion on the Simon effect as reflected by p300. ScientificWorldJournal 2013, 516906. [PubMed: 24459434]

Menardi A, Pascual-Leone A, Fried PJ, Santarnecchi E, 2018. The Role of Cognitive Reserve in Alzheimer's Disease and Aging: A Multi-Modal Imaging Review. J Alzheimers Dis 66(4), 1341–1362. [PubMed: 30507572]

Montagne A, Nation DA, Sagare AP, Barisano G, Sweeney MD, Chakhoyan A, Pachicano M, Joe E, Nelson AR, D'Orazio LM, Buennagel DP, Harrington MG, Benzinger TLS, Fagan AM, Ringman JM, Schneider LS, Morris JC, Reiman EM, Caselli RJ, Chui HC, Tcw J, Chen Y, Pa J, Conti PS, Law M, Toga AW, Zlokovic BV, 2020. APOE4 leads to blood-brain barrier dysfunction predicting cognitive decline. Nature 581(7806), 71–76. [PubMed: 32376954]

Mortamais M, Portet F, Brickman AM, Provenzano FA, Muraskin J, Akbaraly TN, Berr C, Touchon J, Bonafe A, le Bars E, Menjot de Champfleur N, Maller JJ, Meslin C, Sabatier R, Ritchie K, Artero S, 2014. Education modulates the impact of white matter lesions on the risk of mild cognitive impairment and dementia. Am J Geriatr Psychiatry 22(11), 1336–1345. [PubMed: 24021219]

Nakamura A, Cuesta P, Fernandez A, Arahata Y, Iwata K, Kuratsubo I, Bundo M, Hattori H, Sakurai T, Fukuda K, Washimi Y, Endo H, Takeda A, Diers K, Bajo R, Maestu F, Ito K, Kato T, 2018.

Electromagnetic signatures of the preclinical and prodromal stages of Alzheimer's disease. Brain 141(5), 1470–1485. [PubMed: 29522156]

Narbutas J, Egroo MV, Chylinski D, Gonzalez PV, Jimenez CG, Besson G, Ghaemmaghami P, Hammad G, Muto V, Schmidt C, Luxen A, Salmon E, Maquet P, Bastin C, Vandewalle G, Collette F, 2019. Cognitive efficiency in late midlife is linked to lifestyle characteristics and allostatic load. Aging (Albany NY) 11(17), 7169–7186. [PubMed: 31503006]

Nathan PJ, Lim YY, Abbott R, Galluzzi S, Marizzoni M, Babiloni C, Albani D, Bartres-Faz D, Didic M, Farotti L, Parnetti L, Salvadori N, Muller BW, Forloni G, Girtler N, Hensch T, Jovicich J, Leeuwis A, Marra C, Molinuevo JL, Nobili F, Pariente J, Payoux P, Ranjeva JP, Rolandi E, Rossini PM, Schonknecht P, Soricelli A, Tsolaki M, Visser PJ, Wiltfang J, Richardson JC, Bordet R, Blin O, Frisoni GB, PharmaCog C, 2017. Association between CSF biomarkers, hippocampal volume and cognitive function in patients with amnestic mild cognitive impairment (MCI). Neurobiol Aging 53, 1–10. [PubMed: 28189924]

Nombela C, Nombela M, Castell P, Garcia T, Lopez-Coronado J, Herrero MT, 2014. Alpha-theta effects associated with ageing during the Stroop test. PLoS One 9(5), e95657. [PubMed: 24867024]

Nunes RR, Almeida MP, Sleigh JW, 2004. [Spectral entropy: a new method for anesthetic adequacy.]. Rev Bras Anestesiol 54(3), 404–422. [PubMed: 19471748]

Pagano S, Fait E, Monti A, Brignani D, Mazza V, 2015. Electrophysiological Correlates of Subitizing in Healthy Aging. PLoS One 10(6), e0131063. [PubMed: 26098959]

Pan C, Korff A, Galasko D, Ginghina C, Peskind E, Li G, Quinn J, Montine TJ, Cain K, Shi M, Zhang J, 2015. Diagnostic Values of Cerebrospinal Fluid T-Tau and Abeta(4)(2) using Meso Scale Discovery Assays for Alzheimer's Disease. J Alzheimers Dis 45(3), 709–719. [PubMed: 25613100]

Patten RV, Fagan AM, Kaufman DAS, 2018. Differential Cued-Stroop Performance in Cognitively Asymptomatic Older Adults with Biomarker-Identified Risk for Alzheimer's Disease: A Pilot Study. Curr Alzheimer Res 15(9), 820–827. [PubMed: 29623843]

Pettigrew C, Soldan A, Zhu Y, Cai Q, Wang MC, Moghekar A, Miller MI, Singh B, Martinez O, Fletcher E, DeCarli C, Albert M, 2020. Cognitive reserve and rate of change in Alzheimer's and cerebrovascular disease biomarkers among cognitively normal individuals. Neurobiol Aging 88, 33–41. [PubMed: 31932050]

Qi Z, Wu X, Wang Z, Zhang N, Dong H, Yao L, Li K, 2010. Impairment and compensation coexist in amnestic MCI default mode network. Neuroimage 50(1), 48–55. [PubMed: 20006713]

Quandt F, Bonstrup M, Schulz R, Timmermann JE, Zimerman M, Nolte G, Hummel FC, 2016. Spectral Variability in the Aged Brain during Fine Motor Control. Front Aging Neurosci 8, 305. [PubMed: 28066231]

Ranasinghe KG, Cha J, Iaccarino L, Hinkley LB, Beagle AJ, Pham J, Jagust WJ, Miller BL, Rankin KP, Rabinovici GD, Vossel KA, Nagarajan SS, 2020. Neurophysiological signatures in Alzheimer's disease are distinctly associated with TAU, amyloid-beta accumulation, and cognitive decline. Sci Transl Med 12(534).

Riedner BA, Goldstein MR, Plante DT, Rumble ME, Ferrarelli F, Tononi G, Benca RM, 2016. Regional Patterns of Elevated Alpha and High-Frequency Electroencephalographic Activity during Nonrapid Eye Movement Sleep in Chronic Insomnia: A Pilot Study. Sleep 39(4), 801–812. [PubMed: 26943465]

Ritchie C, Smailagic N, Noel-Storr AH, Ukoumunne O, Ladds EC, Martin S, 2017. CSF tau and the CSF tau/ABeta ratio for the diagnosis of Alzheimer's disease dementia and other dementias in people with mild cognitive impairment (MCI). Cochrane Database Syst Rev 3, CD010803. [PubMed: 28328043]

Rochart R, Liu Q, Fonteh AN, Harrington MG, Arakaki X, 2020. Compromised Behavior and Gamma Power During Working Memory in Cognitively Healthy Individuals With Abnormal CSF Amyloid/Tau. Front Aging Neurosci 12, 574214. [PubMed: 33192465]

Roe CM, Fagan AM, Grant EA, Hassenstab J, Moulder KL, Maue Dreyfus D, Sutphen CL, Benzinger TL, Mintun MA, Holtzman DM, Morris JC, 2013. Amyloid imaging and CSF biomarkers in predicting cognitive impairment up to 7.5 years later. Neurology 80(19), 1784–1791. [PubMed: 23576620]

Schneider JA, Arvanitakis Z, Leurgans SE, Bennett DA, 2009. The neuropathology of probable Alzheimer disease and mild cognitive impairment. Ann Neurol 66(2), 200–208. [PubMed: 19743450]

Stam CJ, de Haan W, Daffertshofer A, Jones BF, Manshanden I, van Cappellen van Walsum AM, Montez T, Verbunt JP, de Munck JC, van Dijk BW, Berendse HW, Scheltens P, 2009. Graph theoretical analysis of magnetoencephalographic functional connectivity in Alzheimer's disease. Brain 132(Pt 1), 213–224. [PubMed: 18952674]

Stern Y, 2009. Cognitive reserve. Neuropsychologia 47(10), 2015–2028. [PubMed: 19467352]

Suffczynski P, Kalitzin S, Pfurtscheller G, Lopes da Silva FH, 2001. Computational model of thalamo-cortical networks: dynamical control of alpha rhythms in relation to focal attention. Int J Psychophysiol 43(1), 25–40. [PubMed: 11742683]

Tissier C, Linzarini A, Allaire-Duquette G, Mevel K, Poirel N, Dollfus S, Etard O, Orliac F, Peyrin C, Charron S, Raznahan A, Houde O, Borst G, Cachia A, 2018. Sulcal Polymorphisms of the IFC and ACC Contribute to Inhibitory Control Variability in Children and Adults. eNeuro 5(1).

Tse CS, Balota DA, Yap MJ, Duchek JM, McCabe DP, 2010. Effects of healthy aging and early stage dementia of the Alzheimer's type on components of response time distributions in three attention tasks. Neuropsychology 24(3), 300–315. [PubMed: 20438208]

van Veen V, Carter CS, 2005. Separating semantic conflict and response conflict in the Stroop task: a functional MRI study. Neuroimage 27(3), 497–504. [PubMed: 15964208]

Vazquez-Marrufo M, Galvao-Carmona A, Benitez Lugo ML, Ruiz-Pena JL, Borges Guerra M, Izquierdo Ayuso G, 2017. Retest reliability of individual alpha ERD topography assessed by human electroencephalography. PLoS One 12(10), e0187244. [PubMed: 29088307]

Wilder C, Moncrieffe K, Nolty A, ;, Arakaki X, Fonteh A, Harrington M, 2018. Boston Naming Test predicts deterioration of cerebrospinal fluid biomarkers in pre-symptomatic Alzheimer's disease. The FASEB Journal 32(1_supplement).

Wilson RS, Bennett DA, Gilley DW, Beckett LA, Barnes LL, Evans DA, 2000. Premorbid reading activity and patterns of cognitive decline in Alzheimer disease. Arch Neurol 57(12), 1718–1723. [PubMed: 11115237]

Xavier G, Su Ting A, Fauzan N, 2020. Exploratory study of brain waves and corresponding brain regions of fatigue on-call doctors using quantitative electroencephalogram. J Occup Health 62(1), e12121. [PubMed: 32515890]

Highlights:

- Alpha desynchronization during Stroop test unmasked early amyloid/tau pathology
- Alpha spectral entropy with increasing Stroop load revealed early amyloid/tau pathology
- Alpha desynchronization related to cognitive reserve in early amyloid/tau pathology

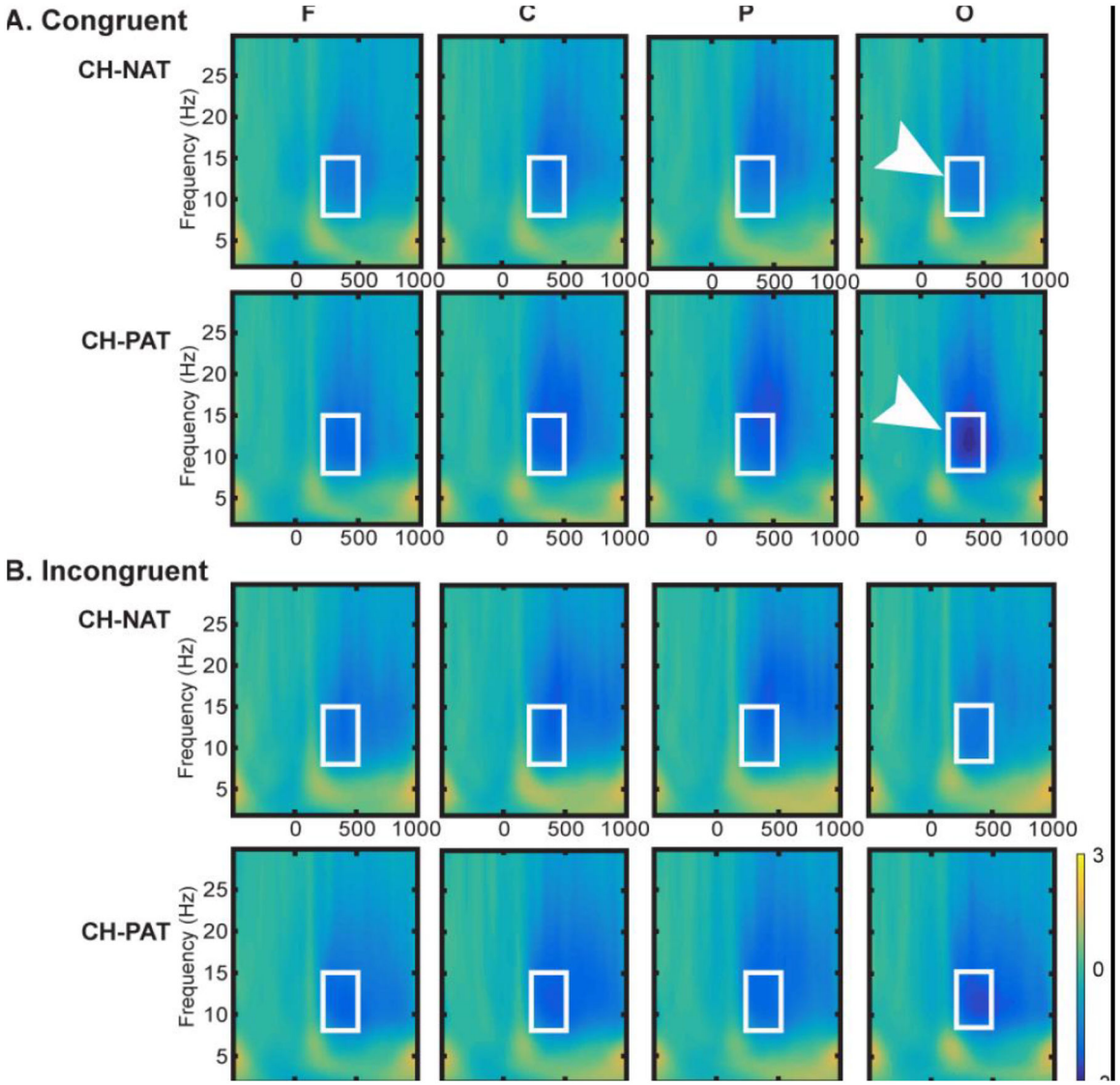

Fig 1. Time-frequency plots (F, C, P, and O regions) of mean Stroop test.

3D plot with time reference to stimulus onset (x-axis in ms, time '0' as stimulus onset), frequency (y-axis in Hz), and power (color scale in dB units) during low load congruent trials (A) and high load incongruent trials (B). The rectangle indicates the representative alpha ERDs (white box with arrowhead) comparing the CH-NAT with the CH-PAT groups in the frontal, central, parietal, and occipital regions. Only during congruent trials (A), alpha ERDs were lower in CH-PAT (−2.11+/−1.32, N=21) vs. CH-NAT (−1.25+/−1.03, N=20) participants in occipital region (p=0.024, ES=−0.84). Column 1 shows power from F = frontal, column 2 C = central, column 3 P = parietal, and column 4 O = occipital, as indicated. ES: effect size.

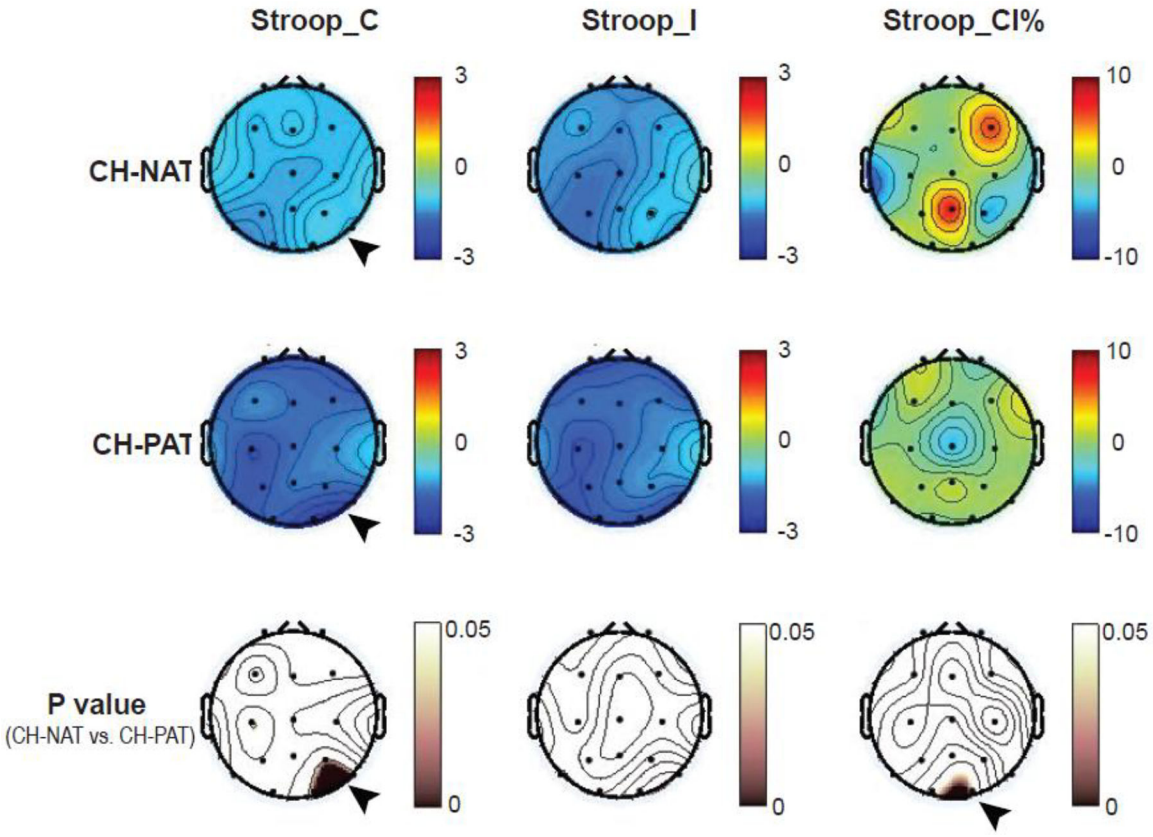

Fig 2. Topoplots of mean alpha ERD during different Stroop interference load (congruent trials and incongruent trials), by groups.

Topo-plots: occipital alpha ERD was more negative in CH-PATs (p=0.024, ES=−0.84, arrowhead) during congruent trials. Alpha ERD during congruent (C, left column) and incongruent (I, middle column) trials and congruent-to-incongruent percentage changes (right column) were shown for CH-NAT (row 1), CH-PATs (row 2), and p values of group comparisons (row 3). Alpha ERD is in dB units based on the colored scale bar on the right; p values are on the bottom row based on the pink scale bar on the right of each plot. ES: effect size.

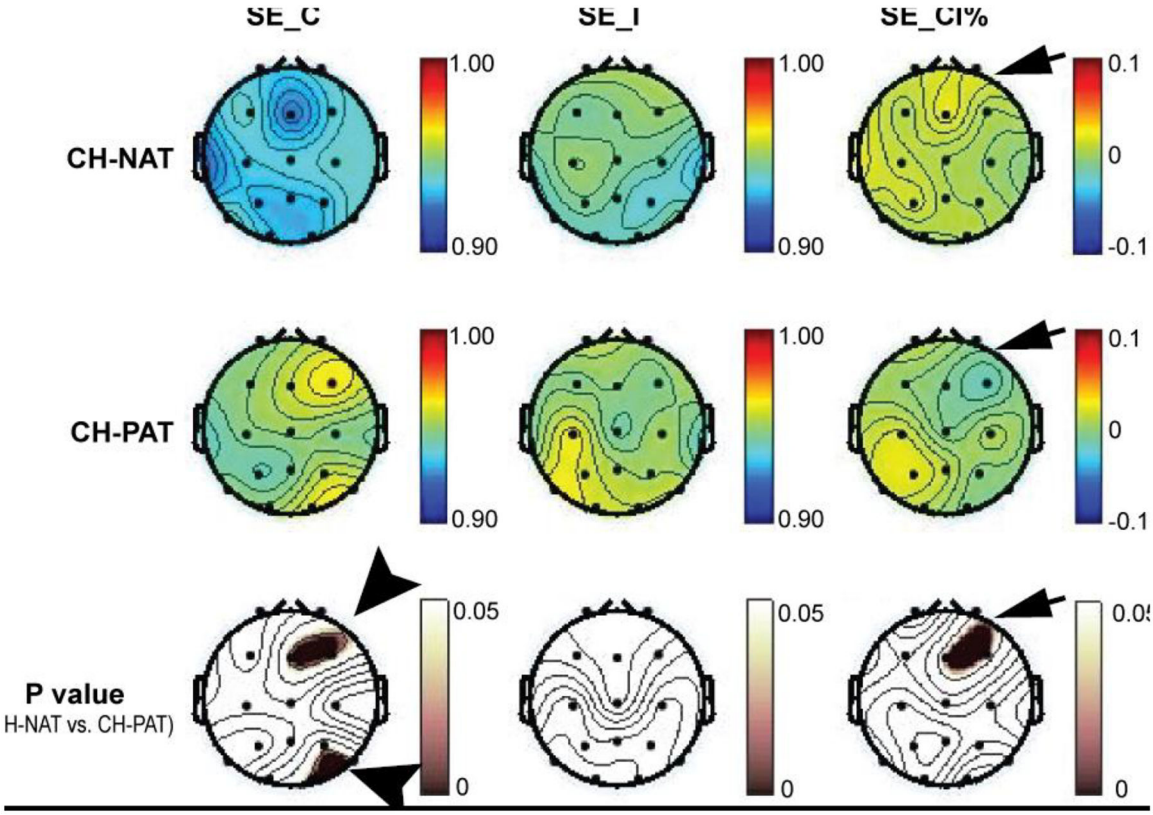

Fig 3. Topoplots of mean alpha SE during active ERD window for congruent (C) and incongruent (I) trials, and changes from C to I trials, by group.

Alpha SE in CH-PATs was lower during congruent trials (F: p=0.042, ES=0.67; O: p= 0.039, ES=0.67, arrowhead) and has smaller changes from congruent to incongruent trials in F region (p=0.012, ES=−0.73, arrows). Alpha SE during congruent (C, left column) and incongruent (I, middle column) trials and congruent-to-incongruent percentage changes (right column) were shown for CH-NAT (top row), CH-PATs (middle row), and p values of group comparisons (bottom row). Alpha SE was shown in values based on the colored scale bar on the right (top two rows); p values were shown on the bottom row based on the pink scale bar. ES: effect size.

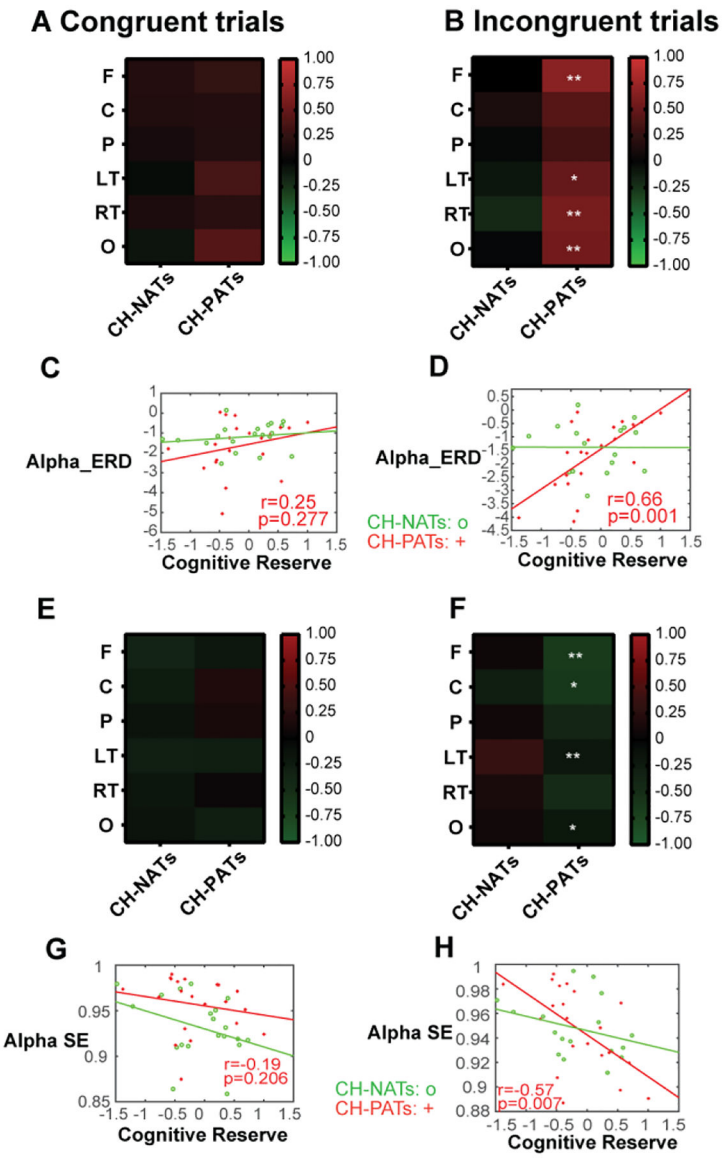

Fig 4. Correlation of alpha ERD with cognitive reserve by groups.

The color maps show the correlation of alpha ERD and cognitive reserve for CH-NATs and CH-PATs for all six brain regions during congruent (A) and incongruent (B) trials. Color indicates r values, *: p<0.05; **: p<0.01; r and p values are not shown when p>0.05. Frontal alpha ERD correlation details are shown for CH-NATs (green circle) and CH-PATs (red cross) during congruent (C) and incongruent (D) trials. For significant correlation (p<0.05), r and p values are shown in corresponding colors: alpha ERD correlated positively with cognitive reserve during incongruent trials for CH-PATs (r=0.66, p=0.001). The correlation of cognitive reserve and alpha SE by groups for brain regions are shown in the color map during congruent (E) and incongruent (F) trials. The color indicates r values. *: p<0.05, **: p<0.01. Frontal alpha SE correlation details are shown for CH-NATs (green circle) and CH-PATs (red cross) during congruent (G) and incongruent (H) trials. Frontal alpha SE

correlated negatively with cognitive reserve during incongruent trials for CH-PATs ($r=-0.57$, $p=0.007$).

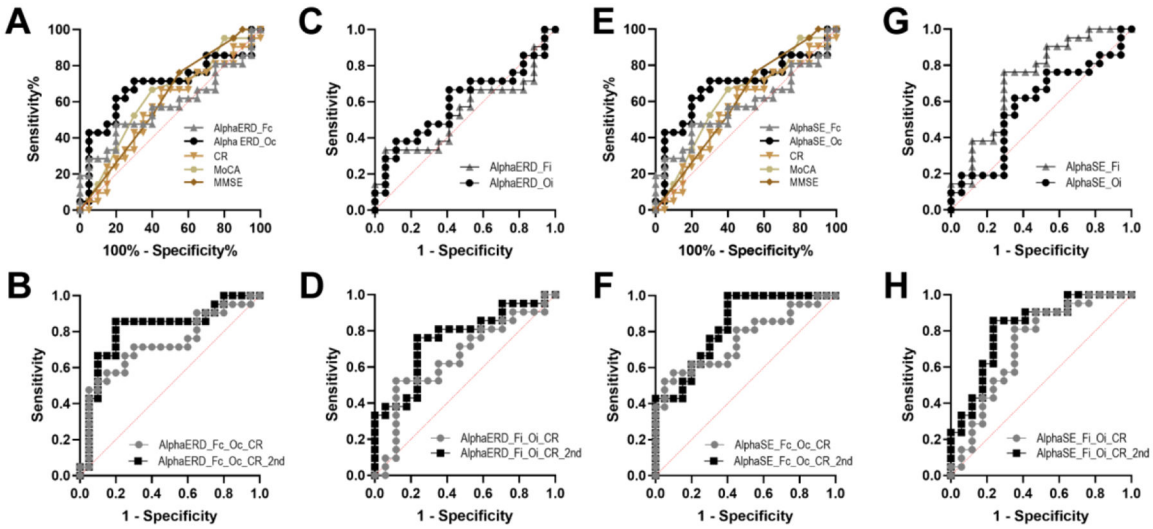

Fig. 5. ROC for CH-NATs vs CH-PATs by alpha ERD/SE and cognitive reserve.

(A) Frontal alpha ERD during congruent trials (Fc) (AUC=0.58, p=0.389), occipital alpha ERD during congruent trials (Oc) (AUC=0.69, p=0.039), cognitive reserve (CR: AUC=0.56, p=0.514), Montreal Cognitive Assessment (MoCA: AUC=0.63, p=0.167), and Mini Mental State Examination (MMSE: AUC=0.61, p=0.241) were different binary classifiers of CH-NATs and CH-PATs. (B) Combination of alpha ERD during congruent trials (Fc and Oc), and cognitive reserve were significant binary classifiers of CH-NATs and CH-PATs (AUC=0.72, p=0.014). They were more significant binary classifiers of CH-NATs and CH-PATs when considering two-way interactions (AUC=0.81, p=0.0006). (C) Frontal alpha ERD during incongruent trials (Fi) (AUC=0.54, p=0.649), occipital alpha ERD during incongruent trials (Oi) (AUC=0.60, p=0.297) were different binary classifiers of CH-NATs and CH-PATs. (D) Combination of alpha ERD during incongruent trials (Fi and Oi), and cognitive reserve were binary classifiers of CH-NATs and CH-PATs (AUC=0.65, p=0.110). They were significant binary classifiers of CH-NATs and CH-PATs when considering two-way interactions (AUC=0.75, p=0.008). (E) Frontal alpha SE during congruent trials (Fc) (AUC=0.73, p=0.012), occipital alpha SE during congruent trials (Oc) (AUC=0.69, p=0.035), cognitive reserve (CR: AUC=0.56, p=0.514), Montreal Cognitive Assessment (MoCA: AUC=0.63, p=0.167), Mini Mental State Examination (MMSE: AUC=0.61, p=0.241) were different binary classifiers of CH-NATs and CH-PATs. (F) Combination of alpha SE during congruent trials (Fc and Oc) and cognitive reserve were significant binary classifiers of CH-NATs and CH-PATs (AUC=0.75, p=0.005). They were more significant binary classifiers of CH-NATs and CH-PATs when considering two-way interactions (AUC=0.83, p=0.0003). (G) Frontal alpha SE change from congruent to incongruent trials (Fci) (AUC=0.72, p=0.020), occipital alpha SE change from congruent to incongruent trials (Oi) (AUC=0.58, p=0.403) were different binary classifiers of CH-NATs and CH-PATs. (H) Combination of alpha SE change from congruent to incongruent trials (Fci and Oci) and cognitive reserve were significant binary classifiers of CH-NATs and CH-PATs (AUC=0.72, p=0.021). They were more significant binary classifiers of CH-NATs and CH-PATs when considering two-way interactions (AUC=0.81, p=0.001). CR: cognitive reserve; MoCA: Montreal Cognitive Assessment. CH-NAT: cognitively healthy

with normal amyloid/tau ratio in cerebrospinal fluid (CSF); CH-PAT: cognitively healthy with pathological amyloid/tau ratio in cerebrospinal fluid (CSF).

Table 1.

Baseline characteristics of participants.

	CH-NAT (n = 20)	CH-PAT (n = 21)	p-value
Age (mean, SD)	75.1 (7.5)	76.2 (8.4)	0.65[&]
Male/Female	5/15	5/16	0.99[#]
Mean Education (SD) (yrs)	15.7 (2.3)	16.3 (1.9)	0.33[&]
R/L/M handedness[*]	16/1/3	19/2/0	0.31[#]
MSD Aβ42 (mean, SD)	292.6 (170.3)	272.9 (181.8)	0.72[&]
MSD pT181 (mean, SD)	53.3 (19.9)	73.9 (32.5)	0.02[&]
MSD Total Tau (mean, SD)	182.8 (172.1)	475.3 (277.6)	2.50E-4[&]
Estimated Innotest Amyloid (mean, SD)	776.8 (251.1)	911.0 (389.2)	0.23[&]
Estimated Innotest Total Tau (mean, SD)	186.4 (113.4)	742.9 (342.2)	1.02E-07[&]
Estimated Innotest Amyloid/total Tau ratio (mean, SD)	4.7 (1.6)	1.4 (0.68)	2.4E-10[&]
MMSE (mean, SD)	29.3 (1.3)	29.2 (0.98)	0.78[&]
vIQ (mean, SD)	124.1 (12.7)	122.7 (15.6)	0.75[&]
Cognitive reserve socre (mean, SD)	−0.04 (0.59)	−0.11 (0.55)	0.72[&]
Total Cholesterol (mean, SD)	184.0 (33.6)	183.4 (37.6)	0.97[&]
HDL (mean, SD)	58.1 (15.5)	70.8 (17.0)	0.07[&]
Smoke (n,%)	11 (55%)	12 (57%)	0.99[#]
Resting SBP (mean, SD)	125.3 (17.1)	131.7 (16.2)	0.23[&]
Resting DBP (mean, SD)	77.2 (9.5)	78.6 (9.0)	0.63[&]

[&]Two-tailed t-test

[#]Fisher's exact test

[*]Freeman-Halton Extension.

Table 2.

Mean (SD) response accuracy (ACC) and response time (RT) in the Stroop test.

	CH-NAT	CH-PAT	T-stat (DF)	p-value
Congruent trials				
N	20	21		
ACC	0.94 (0.03)	0.94 (0.02)	−0.006 (34)	0.995
RT (ms)	784.92 (125.16)	742.66 (98.90)	1.20 (36)	0.240
Incongruent trials				
N	20	21		
ACC	0.90 (0.04)	0.90 (0.05)	0.29 (37)	0.772
RT (ms)	994.57 (186.64)	952.18 (143.23)	0.81 (36)	0.422

* t-test critical value: 1 tail (1.69) 2 tail (2.03); $p < 0.05$. Two-tail t-test

Table 3a.

Comparison of alpha ERD between CH-NAT and CH-PAT during congruent trials.

	CH-NAT (n=20)		CH-PAT (n=21)		DF	T-stat*	Effect Size	P-value
	Mean	SD	Mean	SD				
F	−1.2	0.68	−1.65	1.32	30	1.4	−0.43	0.172
C	−1.26	0.78	−1.77	1.3	33	1.55	−0.48	0.131
P	−1.23	1	−1.77	1.11	39	1.66	−0.52	0.104
LT	−1.17	0.86	−1.74	1.28	35	1.66	−0.51	0.106
RT	−1.1	0.74	−1.68	1.13	35	1.95	−0.60	0.059
O	−1.25	1.03	−2.11	1.32	38	2.35	−0.73	**0.024**

* t-test critical values: 1 tail (1.68) 2 tails (2.02)

Table 3b.

Comparison of alpha ERD between CH-NAT and CH-PAT during incongruent trials.

	CH-NAT (n=17)		CH-PAT (n=21)		DF	T-stat*	Effect Size	P-value
	Mean	SD	Mean	SD				
F	−1.39	0.91	−1.68	1.27	36	0.81	−0.26	0.423
C	−1.5	0.96	−1.75	1.25	36	0.7	−0.22	0.489
P	−1.42	1.15	−1.67	1.03	32	0.71	−0.23	0.485
LT	−1.54	0.9	−1.79	1.26	36	0.72	−0.23	0.473
RT	−1.19	0.75	−1.59	1.12	35	1.31	−0.41	0.198
O	−1.41	1.13	−1.95	1.41	36	1.33	−0.42	0.193

* t-test critical values: 1 tail (1.68) 2 tails (2.02)

Table 3c.

Comparison of alpha ERD changes from congruent to incongruent trials ((I-C)/C) between CH-NAT and CH-PAT.

	CH-NAT (n=17)		CH-PAT (n=21)		DF	T-stat*	Effect Size	P-value
	Mean	SD	Mean	SD				
F	2.13	8.00	−0.03	3.75	22	1.02	−0.36	0.317
C	−0.52	2.46	−1.57	6.30	27	0.70	−0.21	0.488
P	1.43	3.75	0.36	1.33	19	1.12	−0.40	0.276
LT	−1.57	9.78	−0.74	3.00	18	−0.34	0.12	0.741
RT	−1.90	4.78	0.81	2.45	23	−2.12	0.74	0.045
O	0.28	0.59	−0.39	0.93	34	2.68	−0.84	**0.011**

* t-test critical values: 1 tail (1.68) 2 tails (2.02)

Table 4a.

Comparison of alpha ERD between A−T−N− and A+ during congruent trials.

	A−T−N− (n=19)		A+ (n=12)		DF	T-stat*	Effect Size	P-value
	Mean	SD	Mean	SD				
F	−1.31	1.16	−1.39	0.95	25	0.23	−0.07	0.848
C	−1.41	1.15	−1.31	1.15	22	−0.06	0.08	0.824
P	−1.44	1.17	−1.25	0.93	25	−0.43	0.18	0.638
LT	−1.46	1.21	−1.22	0.95	25	−0.49	0.21	0.572
RT	−1.30	0.90	−1.27	0.84	23	0.04	0.04	0.920
O	−1.50	1.26	−1.43	1.00	25	−0.13	0.06	0.871

* t-test critical values: 1 tail (1.68) 2 tails (2.02)

Table 4b.

Comparison of alpha ERD between A−T−N− and A+ during incongruent trials.

	A−T−N− (n=16)		A+ (n=12)		DF	T-stat*	Effect Size	P-value
	Mean	SD	Mean	SD				
F	−1.49	1.18	−1.53	1.24	21	0.06	−0.03	0.929
C	−1.69	1.40	−1.35	1.05	24	−0.72	0.27	0.482
P	−1.61	1.27	−1.28	1.08	23	−0.91	0.28	0.476
LT	−1.77	1.28	−1.34	0.97	24	−0.89	0.37	0.339
RT	−1.36	0.95	−1.31	1.03	21	−0.08	0.05	0.895
O	−1.50	1.34	−1.60	1.23	23	0.2	−0.08	0.839

* t-test critical values: 1 tail (1.68) 2 tails (2.02)

Author Manuscript

Author Manuscript

Author Manuscript

Table 4c.

Comparison of alpha ERD changes from congruent to incongruent trials ((I-C)/C) between A−T−N− and A+.

	A−T−N− (n=16)		A+ (n=12)		DF	T-stat*	Effect Size	P-value
	Mean	SD	Mean	SD				
F	1.33	9.10	1.20	2.87	18	0.05	−0.02	0.962
C	−2.47	7.33	−0.23	1.91	16	−1.07	0.39	0.313
P	1.41	3.84	0.68	1.82	23	0.44	−0.23	0.549
LT	−0.03	1.53	−0.15	4.89	11	0.11	−0.04	0.923
RT	−0.31	2.30	0.72	2.87	19	−1.03	0.40	0.304
O	−0.17	1.10	0.04	0.75	24	−0.55	0.22	0.566

* t-test critical values: 1 tail (1.68) 2 tails (2.02)

Table 5a.

Comparison of alpha SE between CH-NAT and CH-PAT during congruent trials.

	CH-NAT(n=20)		CH-PAT(n=21)		DF	T-stat*	Effect Size	P-value
	Mean	SD	Mean	SD				
F	0.93	0.03	0.96	0.03	38	−2.49	0.78	**0.017**
C	0.94	0.03	0.95	0.04	39	−1.21	0.38	0.234
P	0.93	0.04	0.95	0.04	39	−1.4	0.44	0.168
LT	0.93	0.03	0.94	0.03	39	−1.5	0.47	0.141
RT	0.94	0.03	0.95	0.03	38	−1.77	0.55	0.085
O	0.93	0.04	0.96	0.03	38	−2.43	0.76	**0.020**

* t-test critical values: 1 tail (1.68) 2 tails (2.02)

Table 5b.

Comparison of alpha SE between CH-NAT and CH-PAT during incongruent trials.

	CH-NAT(n=17)		CH-PAT(n=21)		DF	T-stat*	Effect Size	P-value
	Mean	SD	Mean	SD				
F	0.95	0.02	0.95	0.03	36	0.03	−0.01	0.976
C	0.95	0.03	0.95	0.03	32	−0.82	0.27	0.419
P	0.94	0.03	0.95	0.03	32	−1.28	0.42	0.209
LT	0.95	0.03	0.95	0.02	32	−0.55	0.18	0.589
RT	0.94	0.03	0.95	0.03	36	−0.82	0.26	0.417
O	0.94	0.04	0.96	0.03	28	−1.52	0.51	0.14

* t-test critical values: 1 tail (1.68) 2 tails (2.02)

Table 5c.

Comparison of alpha SE changes from congruent to incongruent trials ((I-C)/C) between CH-NAT and CH-PAT.

	CH-NAT(n=17)		CH-PAT(n=21)		DF	T-stat*	Effect Size	P-value
	Mean	SD	Mean	SD				
F	0.01	0.03	−0.01	0.02	27	2.55	−0.87	**0.012**
C	0.01	0.03	0.01	0.03	36	0.15	−0.05	0.887
P	0.01	0.05	0.01	0.04	33	0.15	−0.05	0.879
LT	0.02	0.04	0.01	0.03	28	0.85	−0.29	0.381
RT	0	0.05	0	0.03	25	0.63	−0.22	0.509
O	0.01	0.02	0	0.02	34	0.6	−0.20	0.548

* t-test critical values: 1 tail (1.68) 2 tails (2.02)